



Application of Novel Hybrid Membranes in Alkaline Direct Methanol Fuel Cells

RUI DONG^{1,*}, JIANXUN ZHANG², BINGQIAN ZHOU² and PENG FU³

¹School of Chemical and Biological Engineering, Yancheng Institute of Technology, Yancheng 224051, Jiangsu Province, P.R. China

²School of Materials Science and Engineering, Changzhou University, Changzhou 213164, Jiangsu Province, P.R. China

³School of Faculty of Science, Nanjing University of Technology, Nanjing 211816, Jiangsu Province, P.R. China

*Corresponding author: Tel: +86 13382605090; E-mail: dongr@ycit.cn

Received: 29 March 2014;

Accepted: 6 June 2014;

Published online: 4 February 2015;

AJC-16782

A new hybrid anion-exchange membrane with a stable size and dense microstructure was developed. This membrane comprised with quaternized poly(vinyl alcohol) (QPVA), poly(dimethyl diallyl ammonium chloride) (PDADMAC) and tetraethyl orthosilicate (TEOS). The evaluated properties results indicated that the performance of QPVA/0.25PDADMAC/0.1TEOS had many advantages over those of Nafion-series membranes. For example, its methanol content was 37.3 %, which was lower than that of Nafion-115 (41.8 %) at room temperature. The ion-exchange capacity and methanol permeability of the membrane were 1.09 mmol/g and 2.8×10^{-6} cm²/s, respectively, which were distinct from that of Nafion-117 whose values were 0.91 mmol/g and $(4.5-9.2) \times 10^{-6}$ cm²/s, respectively. Furthermore, the ion conductivity of the membrane reached 5.28×10^{-3} S/cm, whereas the heat stability within 65-140 °C was excellent. All these results illustrated that this new hybrid membrane may have potential applications in alkaline direct methanol fuel cells at low temperatures.

Keywords: Quaternized poly(vinyl alcohol), Poly dimethyl diallyl ammonium chloride, Tetraethyl orthosilicate.

INTRODUCTION

A direct methanol fuel cell (DMFC) is a kind of an environment-friendly power source with high efficiency¹. Ion-exchange membranes have been developed for several main applications *e.g.*, adsorptive removal of anionic dyes² and heavy metal ions³, electrodialysis⁴, acid recovery⁵, pervaporation⁶ and medical uses⁷⁻⁹. These membranes are also used for alkaline direct methanol fuel cells (ADMFCs)¹⁰⁻¹⁵.

Numerous studies have already been conducted on the preparation of anion-exchange membranes. All ordinary routes can be summarized into four, as follows:

(1) The quaternization following the chloromethylation of aromatic polymers acting as base materials, as described by Dong and co-workers¹⁶. They synthesized anion-exchange membranes with outstanding ionic conductivities through the chloromethylation of polysulfone, followed by the optimized quaternization. However, chloromethyl methyl ether as a cationic etherifying agent is highly carcinogenic¹⁵. Previous workers¹² were also able to prepare guanidine cationic anion-exchange membranes exhibiting excellent stabilities based on polyether sulphone, but their process, which used chloromethyl methyl ether, deals harm to operators and the environment.

(2) The quaternization of the pre-synthesized amino-containing materials, which was reported by Fang *et al.*¹⁷.

Polyimide with an amino on its backbone was obtained by the reaction of 5-aminoisophthalic acid with 3,3-diaminobenzidine. Simultaneously, epichlorohydrin and 4-methylmorpholine reacted in acetonitrile for 48 h to get the quaternized intermediate 4-methyl-4-glycidylmorpholin-4-ium chloride. The polyimide-based anion-exchange membranes were synthesized through the grafting and cross-linking reactions of the two above mentioned products prepared in advance. Although this method eliminated the use of chloromethyl methyl ether, its multiple synthesis steps, long reaction time and the involvement of certain toxic agents were its main limitations. By ring-opening metathesis polymerization (ROMP), Clark *et al.*¹⁸ prepared a kind of anion-exchange membranes functionalized with quaternary ammonium groups. First, 1,3-cyclopentadiene and methacrylaldehyde reacted in methylene chloride solution containing 10 % mol boron trichloride at -50 °C for 1.5 h. Second, dimethylamine was added to react with tertiary amine groups for another 16 h at 20 °C. The quaternary ammonium groups were then attached onto the polymer in the acetone solution through the addition of methyl iodide for 16 h to produce the target monomer. In the presence of the Grubbs second generation catalyst, the ring-opening metathesis polymerization of the monomer and dicyclopentadiene (DCPD) in trichloromethane and the subsequent alkalization in the KOH all worked to yield the novel quaternary ammonium-

based anion-exchange membranes. However, the above process was too complex and several irritant drugs harmful to the environment were also used.

(3) The copolymerization of compounds containing cationic functional groups and conventional polymers for the formation of new alkaline anion-exchange membranes, as reported by Kostalik *et al.*¹⁹. The preparation of these alkaline anion-exchange membranes combined the ring-opening copolymerization under the effect of the Grubbs second catalyst and the hydrogenation reduction promoted by the crabtree catalyst of cyclooctene, the materials which contained quaternary ammonium salt cationic and the alkaline effect on iodine ion. The reliance of this technique on new catalysts primarily limited its success. On the other hand, Fang *et al.*¹⁷ utilized 1-allyl trimethyl imidazole chloride salt and methyl acrylate to conduct radical copolymerization in synthesizing anion-exchange membranes with imidazolium cation by the initiation of AIBN. Large-scale application of this technique was hindered by the difficulty of securing imidazole cation compounds.

(4) The grafting reaction of water-soluble polymer and cationic etherifying agent, such as the QPVA of Xiong *et al.*²⁰, which was formed by the grafting of PVA with EPTAC as cationic etherifying agent to yield QPVA and the eventual cross-linking with glutaraldehyde. The procedures involved were eco-friendly, but the stability of the membranes was poor.

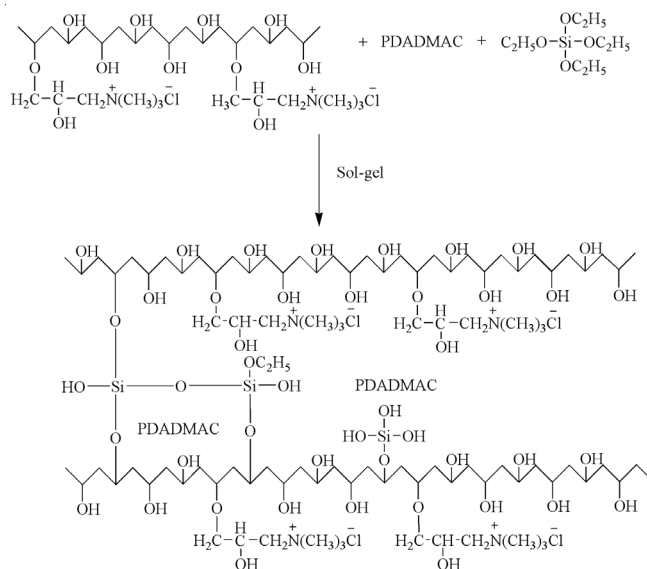
This study aimed use environmental-friendly methods and low-cost materials in obtaining anion-exchange membranes with stable performance and optimal ion conductivity. In this paper, novel hybrid membranes (QPVA/PDADMAC/TEOS) were prepared through the introduction of PDADMAC cationic polymers to the sol-gel network of QPVA, together with TEOS. The application potential of the hybrid anion-exchange membranes was evaluated in ADMFC.

EXPERIMENTAL

Hybrid membrane preparation: Poly(vinyl alcohol) AH-26 and glutaric dialdehyde (25 wt. % water solution) were supplied by Sinopharm Chemical Reagent Co., Ltd. 3-Chloro-2-hydroxypropyl-trimethylammonium chloride was purchased from the Shanghai Bangcheng Chemical Co., Ltd. Poly dimethyl diallyl ammonium chloride (PDADMAC, 20 wt. % water solution) was purchased from the Sigma-Aldrich. Tetraethoxysilanes (TEOS) was purchased from the Aladdin reagent. All the other materials were commercial products and used as received. Quaternized poly(vinyl alcohol) (QPVA) was synthesized in the following conditions: the mole ratio of 3-chloro-2-hydroxypropyl-trimethylammonium chloride and the hydroxy groups in poly(vinyl alcohol) was 1.4:1, reacted at 65 °C for 5 h.

A sufficient amount of QPVA was added to deionized water and the mixture was continuously stirred until swelling. The 10 wt. % casting solution was obtained after the sufficient dissolution of QPVA as the temperature gradually rised to 80 °C. Likewise, 8 wt. % PDADMAC casting solution was prepared by dissolving PDADMAC in deionized water with magnetic stirring at room temperature. Both of the two solutions were mixed on the basis of their mass ratio marked as QPVA/ χ PDADMAC (where χ is the mass ratio of PDADMAC and QPVA casting solutions with values of 0, 25, 50, 75 and

100 %), while keeping the total mass fixed at 20 g. Subsequently, the pH of the mixture was adjusted to 3 by the addition of 0.1 mol/L HCl. Tetraethyl orthosilicate (0.2 g) was added dropwise to the mixture with magnetic stirring for 1 h at 30 °C. Through ultrasonic deaeration, the mixture became an apparent sol-gel solution. A given volume of mixture was poured onto a homemade mould and dried. In the end, hybrid anion-exchange membranes with varying intensities were produced. The preparation route is shown in **Scheme-I**.



Scheme-I: Preparation route of QPVA/PDADMAC/TEOS hybrid membranes by sol-gel reaction

The hybrid membranes with varying mass ratios were tailored to several well-controlled size (approximately 2 × 2 cm) membranes and immersed into a 5 wt. % glutaraldehyde/acetone solution and cross-linked at 30 °C, pH 5 for 5 h. The cross-linking solution absorbed on their surfaces was removed and they were immersed into 1 mol/L NaOH solution for 24 h to get the alkaline membranes. Subsequently, the membranes had another round of immersion, this time in deionized water for another 24 h for the subsequent tests.

Structural characterization: The FTIR absorption spectra of QPVA and hybrid membranes were recorded using a NEXUS-670 spectrophotometer. The membrane morphologies were investigated with a QUANTA200 scanning electron microscope (SEM). During microscopy, the samples were quenched in liquid nitrogen, fractured and coated with gold powder. The cross sections were observed and the energy spectra of the regions of interest were analyzed. TG thermal analyses were carried out using a STA449C TG-DSC (NETZSCH, Germany) system. The measurements were conducted by heating the sample from room temperature to 600 °C at a heating rate of 10 °C/min under a nitrogen atmosphere.

Water/methanol content and ion-exchange capacity (IEC): The water/methanol contents of the samples were measured by the dry-wet method. The alkaline membranes were dried under vacuum for 24 h and weighed (W_1). After being immersed in deionized water with methyl alcohol for 24 h, the excess surface solution was removed and the weights of the wet membranes (W_2) were promptly determined. The

water/methanol content W_0 of the membranes was given by the following equation:

$$W_0 = \frac{W_2 - W_1}{W_1} \times 100 \% \quad (1)$$

where W_2 is the mass (g) of a wet membrane and W_1 is the mass (g) of a dry membrane.

The ion exchange capacities of the alkaline anion-exchange membranes were measured using the classical titration method. Each of the alkaline membranes with weight m was immersed in a required volume (V) and concentration (C_0) of the HCl solution and equilibrated for 48 h. With phenolphthalein as the indicator, the back titration using 0.01 mol/L NaOH solution was not halted until the above solutions exhibited a red colour for 30 s. The residual HCl concentration was recorded as C_1 . Ion-exchange capacity was obtained from the following equation:

$$IEC = \frac{(C_0 - C_1) \times V \times 1000}{m} \quad (2)$$

where C_0 and V are the initial concentration and volume of the HCl solution, respectively; C_1 is the residual HCl concentration and m is the mass (g) of each membrane.

Methanol permeability: The methanol permeability was measured using a diffusion cell comprising two compartments (denoted as I and II) and circular silicone cushions with round holes in the middle. First, different alkaline membranes were positioned in between the cushions. I was loaded with 3 mol/L methanol and 0.5 mol/L KOH solution, in amounts of 30 mL each. Meanwhile, II contained only 60 mL deionized water. Both compartments had stirrers and were sealed with preservative films. Last, the methanol permeability (P_M) was examined at 30, 40, 50 and 60 °C. Methanol permeability was obtained through the equation:

$$\text{Methanol permeability} = KV_2d/AC_0 \quad (3)$$

where K is the slope ($\text{mol L}^{-1} \text{S}^{-1}$) of the curve of methanol concentration *vs* time, V_2 is the volume (mL) of the deionized water in II, d is the membrane thickness (cm), A is the area (cm^2) of the membrane and C_0 is the initial concentration (mol/L) of methanol inside I.

The methanol concentration of II compartment was determined by the vapor phase method, which used 0.2 mol/L acetone solution as the internal control. One mL solution in II compartment was mixed with 0.2 mol/L acetone solution of the same volume at prescribed time intervals. At each mixing, 0.5 μL of the mixed solution was assigned as the sample. The methanol concentration of II compartment was measured using SP-6800A gas chromatograph (Rainbow Chemical Instrument Co., Ltd. SHANDONG LUNAN) equipped with a FFAP chromatographic column. The column temperature was set at 100 °C, whereas the sample injection and the tests were all carried out at 150 °C.

Ionic conductivity: Ionic conductivity, which had a crucial effect on the service efficiency of the membranes, was confirmed on Versa STAT3 constant potential rectifier. The device was composed of Versastudio software AC impedance and two stainless steel electrodes. During the testing, membranes were immersed in deionized water to keep the relative humidity to 100 %. The impedance spectrum was obtained and fitted by

Zsimpwin software to obtain the resistance value. The ionic conductivity of the membranes at different temperatures were calculated using the following equation:

$$\sigma = \frac{L}{A \times R} \quad (4)$$

where L is the distance between the two electrodes (*i.e.* the thickness of a membrane (cm)), A is the effective area (cm^2) of a membrane for resistance measurement, R is the resistance value (Ω) and σ is the ionic conductivity (S cm^{-1}).

RESULTS AND DISCUSSION

Structure characteristic of the hybrid membranes:

Compared to QPVAm, the characteristic absorption peak of hydroxyl groups on the chain of QPVA/0.1TEOSm is relatively higher at 3400 cm^{-1} , as shown in Fig. 1. Such phenomenon could be attributed to the sol-gel structure formed in QPVA as TEOS was added. Particularly, a new peak at 1000 cm^{-1} , which belongs to the Si-O bonds, emerged²². Because of the synergic effect of Si-O and C-O bonds, their characteristic absorption peak around 1100 cm^{-1} is markedly different from that of QPVAm. Because of the combined effect of PDADMAC and the cations of QPVA, the peaks of quaternary ammonium groups at 1647 cm^{-1} were all present in the four membranes. However, the peaks of QPVA/0.25PDADMAC/0.1TEOSm were the strongest, indicating that it has a comparatively high ionic exchange capacity.

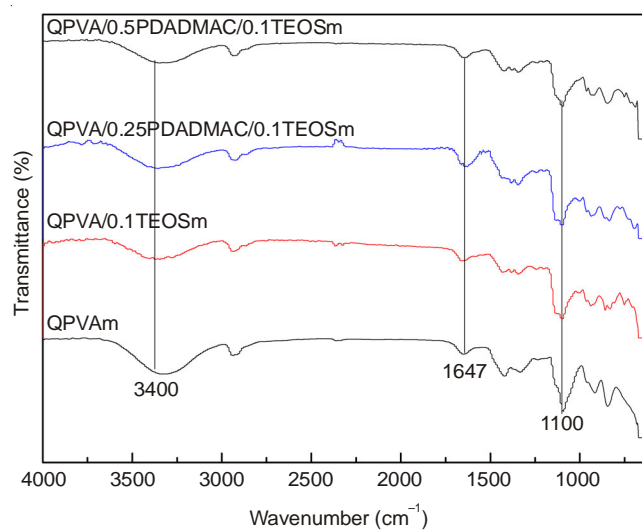


Fig. 1. ATR-FTIR spectrum of different membranes

Morphology analyses of the alkaline membranes: The surfaces ($\times 4000$) and cross-sections ($\times 2400$) of the four hybrid membranes were observed by SEM. Together with the energy spectrum analyses, the types of potential elements can be identified and confirmed.

Fig. 2 distinctly depicts the appearances of the four hybrid alkaline membranes, *i.e.* QPVAm (Type A), QPVA/0.1TEOSm (Type B), QPVA/0.25PDADMAC/0.1TEOSm (Type C) and QPVA/0.5PDADMAC/0.1TEOSm (Type D). The numbers 1 and 2 stand for the surface and the cross-section images, respectively. A1 and A2 were compact without the obvious existence of pores and channels and the white matter present

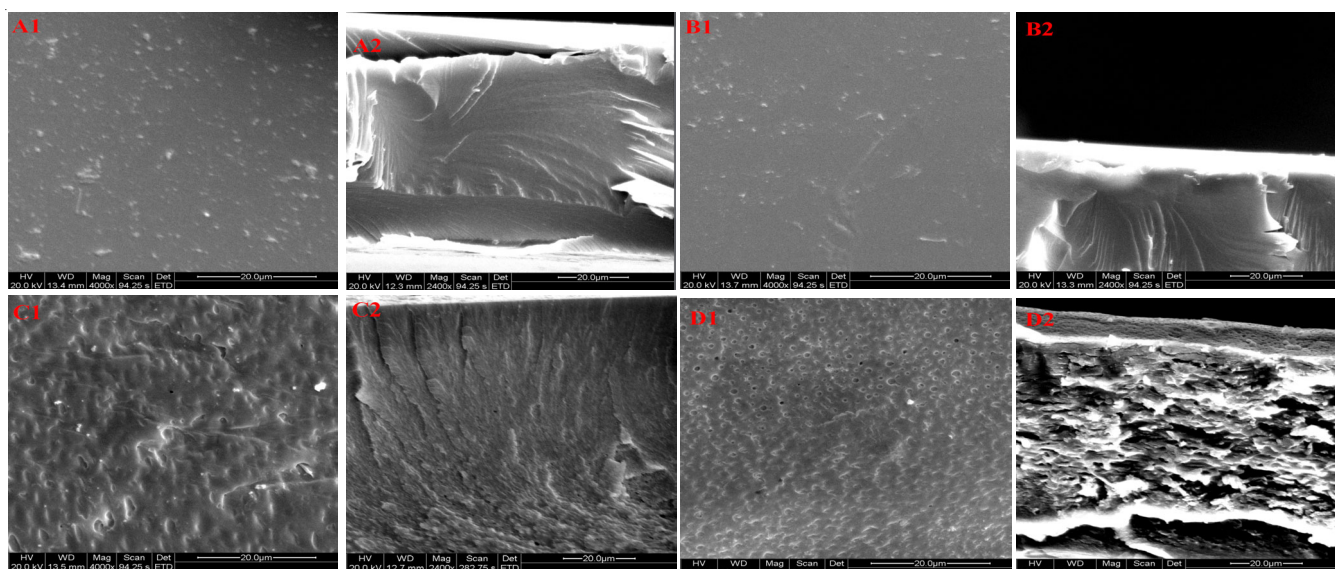


Fig. 2. Surface and cross-section diagrams of different membranes

indicates the grafting of the quaternary ammonium groups on PVA^{23,24}. As a consequence of the addition of TEOS, the membranes became dense. B1 and B2 were dense, but the amount of white materials on B1 was less than that of A1. The random distribution of Si on the surfaces of membranes, affirmed through energy spectrum analysis, proved the existence of the sol-gel network. C1 and C2 had "orange peel-like" tissues, unlike the smooth surfaces of A1 or B1. This observation was caused by the diversity of the compatibility between PDADMAC cation polymer and QPVA that contributes to the microphase separation on the surfaces²⁴. Despite their fracture surfaces being dense, a decent quantity of PDADMAC is constrained into the sol-gel structure. D1 and D2 had similar surfaces *vis-à-vis* that of C1 and C2, but their cross-sections exhibited a "honeycomb" appearance. Such form was caused by the excess PDADMAC cation polymer that brings about the deterioration of the compatibility and the distinct phase separation that decreases the barrier property of the membranes.

Thermal stability: Fig. 3 shows the thermal weight loss of the four types of dry alkaline membranes at the temperature range of 0-600 °C. At around 100 °C, the main loss of the membranes was bound water. Compared with A, the heat-resistance of B increased during the presence of a few TEOS between 0 and 290 °C. At 250-290 °C, thermal stability of B was ascribed to the quaternary ammonium groups which were bound by the sol-gel network and resulted in the delay in the thermal decomposition of the quaternary ammonium group. However, their actual degradation occurred at around 300 °C. At above 395 °C, the formation of the sol-gel network also played an important role on the thermal stability of B. The elimination of hydroxyl groups in the polymer chains began at 352 °C and the polymer segments were disrupted up to 420 °C²¹. In contrast to D, the appreciable thermal stability of C appeared in the range of 65 to 140 °C, primarily because of the overdose of PDADMAC. This activity caused the relative content of QPVA to decrease and the hydroxyl groups for cross-linking to decline. The loose structure and weak thermostability,

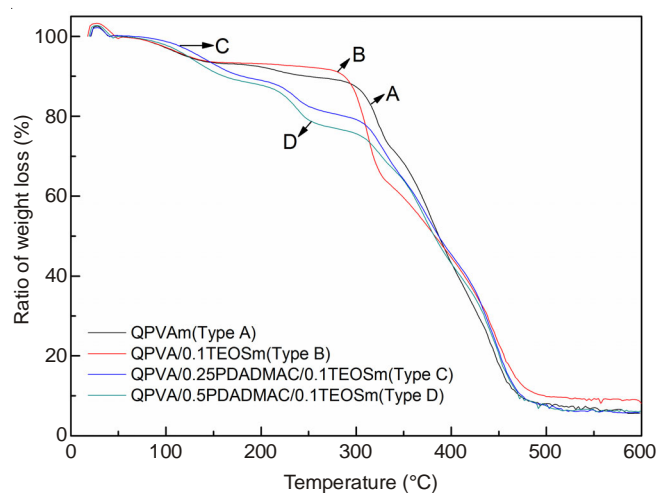


Fig. 3. TGA graphs of different membranes

were induced by the degree of cross-linking of the hybrid alkaline membranes.

Effect of the ratio of water and methanol: Fig. 4 displays the water/methanol ratio of four alkaline membranes QPVAm (Type 1), QPVA/0.1TEOSm (Type 2), QPVA/0.25PDADMAC/0.1TEOSm (Type 3) and QPVA/0.5PDADMAC/0.1TEOSm (Type 4) equilibrated in water/methanol solution. The methanol content was observed to be always lower than the water content, because pristine PVA membrane is hydrophilic and this hydrophilic nature is further reinforced through quaternization. The bound quaternary ammonium groups introduced in membrane 2 due to TEOS made the water content to drop slightly. However, in contrast with the later three membranes, the water/methanol ratio exhibits a similar trend as the content growth of PDADMAC, the water-soluble polymer. The SEM results (Fig. 2) indicate that PDADMAC is present in excess and can cause the emergence of a "honeycomb" pore structure, thereby also leading to a high water/methanol ratio. The increasing water content can facilitate the electrical conductivity of the hydroxyl groups of the membranes, but too much of it can

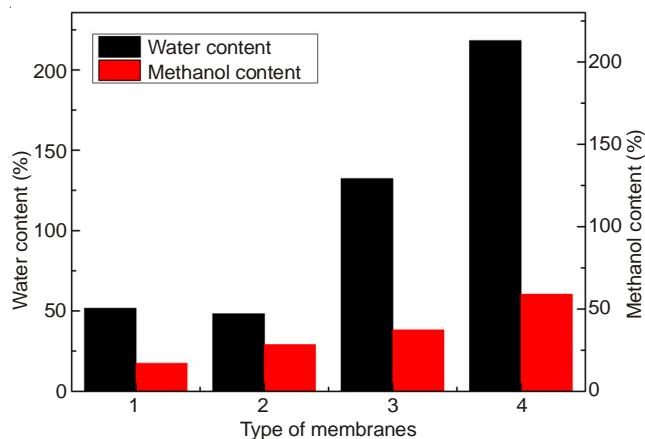


Fig. 4. Water-to-methanol ratio of different membranes

cause an adverse effect on the dimensional stability and the relative concentration of the hydroxyl groups. Hence, the methanol ratio should be set in such a way that the dimensional stability in ADMFC is maintained. QPVA/0.25PDADMAC/0.1TEOSm, which obtained a methanol content (37.3 %) lower than that of Nafion -115 membrane (41.8 %) at room temperature, has potential applications in methanol fuel cells²⁵.

Ion-exchange capacity: The ion exchange capacity of the membranes is one of the significant indexes in evaluating exchangeable groups. The ion-exchange capacity values obtained by back titration are listed in Table-1. The reduction of ion-exchange capacity of membrane B is attributed to the network of TEOS and QPVA formed in the sol-gel reaction, restraining cation quaternary ammonium groups *versus* A. Such activity is consistent with the experimental results on its thermal stability and water absorption capacity. The presence of PDADMAC promotes ion-exchange capacity, but its over-dosage leads to the reverse effect. The excess PMADMAC generates poor pore structure and causes the high absorption of water, thus leading to the decline in ion exchange ability and the relative concentration of functional cationic quaternary ammonium groups. The ion-exchange capacity of QPVA/0.25PDADMAC/0.1TEOSm reached up to 1.09 mmol/g, compared with the commercial Nafion-117 membranes that exhibited only 0.91 mmol/g¹³.

TABLE-1
ION-EXCHANGE CAPACITY OF THE
FOUR STABILITY MEMBRANES

Types of membranes	Ion exchange capacity (mmol/g)
A (QPVA _m)	0.70
B (QPVA/0.1TEOS _m)	0.68
C (QPVA/0.25PDADMAC/0.1TEOS _m)	1.09
D (QPVA/0.5PDADMAC/0.1TEOS _m)	0.68

Methanol permeability: Methanol was dissolved in water to get solutions with concentrations of 0.01, 0.03, 0.05, 0.07 and 0.09 mol/L. Through the measurement of the gas phase of the mixture of 1 mL methanol and 1 mL 0.2 mol/L acetone solution, the standard curve of their peak areas and molar ratios was determined to calculate the unknown concentration of methanol. This curve is shown in Fig. 5 and its linear fitting equation is $Y = 0.60926X + 0.00488$ (Y is the ratio of the peak

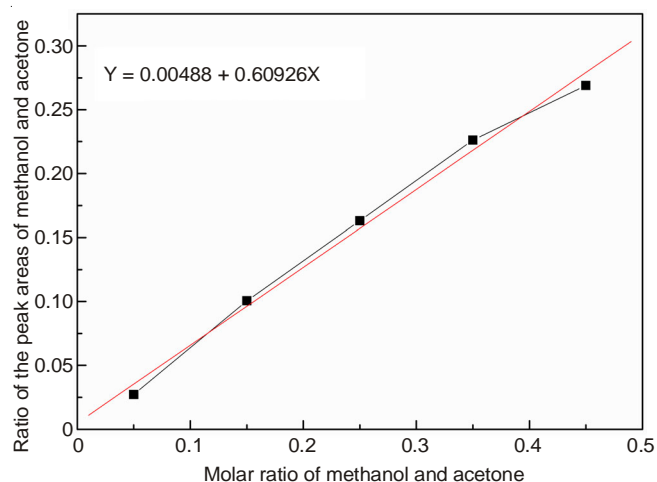


Fig. 5. Standard curve of molar ratio and gas-phase peak areas of methanol and acetone

areas of methanol and acetone and X is the molar ratio of methanol and acetone). According to the methanol concentration at a given temperature and time, the gradient K can be determined. Moreover, the membrane thickness was confirmed by a micrometer and the round pore area was calculated as the membrane face.

In testing methanol resistance, QPVA/0.5PDADMAC/0.1TEOSm suffered with the loose structures of its surface and cross-section, making methanol diffusion as its primary hurdle as a barrier material. In the present study, its methanol permeability was disregarded.

The other three membranes had some extent of methanol-rejection property. The methanol peak signal emerges asynchronously through the gas chromatography testing of the samples in the II compartment. The time sequence was observed, QPVA/0.25PDADMAC/0.1TEOSm emerged as the first and QPVA/0.1TEOSm was the last.

Fig. 6 illustrates the methanol permeability of QPVA_m, QPVA/0.1TEOS_m and QPVA/0.25PDADMAC/0.1TEOS_m. Their permeability increased along with temperature and this trend results from the severe movement of the intermolecular segments, the growing free volume and the strong kinetic energy of methanol. The methanol permeability (referred to as methanol crossover from anode to cathode) of QPVA/0.1TEOS_m was superior than that of QPVA_m, since the sol-gel network formed between TEOS and QPVA made the interaction of the molecular chains more compact and hindered the diffusion of the methanol molecules. Furthermore, methanol permeability was closely correlated with the membrane morphology. When the addition of PDADMAC was 0.25 of the weight of QPVA, the type of membrane produced exhibited a slight exclusion among the molecular chains of the hybrid membranes. SEM results indicate that the surface becomes "orange peel-like", but the side remains dense. Hence, its resistance performance was optimal compared with that of Nafion-117 membrane [$(4.5-9.2) \times 10^{-6} \text{ cm}^2/\text{s}$]^{26,27}. In fuel cells, the resultant OH⁻ anions cross from cathode to anode in a direction opposite to the direction of methanol, thus enhancing the osmotic resistance of methanol. Under electro-dialytic condition, methanol permeability declines further.

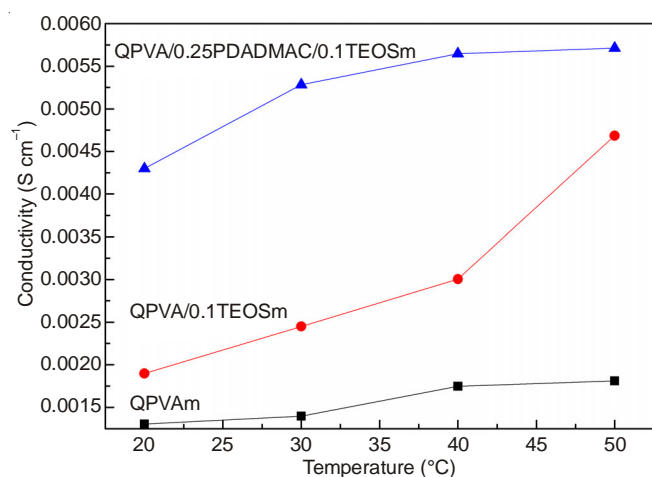


Fig. 6. Relation of the methanol permeability and the temperature of the three membranes

Ionic conductivity analysis: The ionic conductivity of the three membranes of interest (*i.e.*, QPVA, QPVA/0.1TEOSm and QPVA/0.25PDADMAC/0.1TEOSm) determined at 20, 40, 60 and 80 °C are shown in Fig. 7. The ionic conductivity exhibited a similar trend with temperature. At high temperature, the stronger segmental motion of the polymer chains and the larger free volume render the easy OH⁻ transmission. In addition, the ion activity, which accelerates ionic conductivity, must be taken into account. The results had a lot in common with that of ionic conducting materials²⁸. The QPVA/PDADMAC/TEOS hybrid membranes (1/0.25/0.1 in mass ratio) experienced a remarkable increase in their ionic conductivity because the number of quaternary ammonium groups embedded on them is conducive to the crossover of the ions. In contrast, the ionic conductivity of QPVA is greater than that of QPVA/0.1TEOSm, which has a high affinity with the water. In general, the water in the membranes can be classified as free water and bound water²⁸. With respect to OH⁻ transmission, only free water participates in the process, while bound water becomes a barrier²⁹. Moreover, the sol-gel network formed in the presence of TEOS can hold more free water²² at elevated temperature, requiring the transport of OH⁻ anions. The ionic conductivity of QPVA/0.1TEOSm at 50 °C increases high as plotted in Fig. 7.

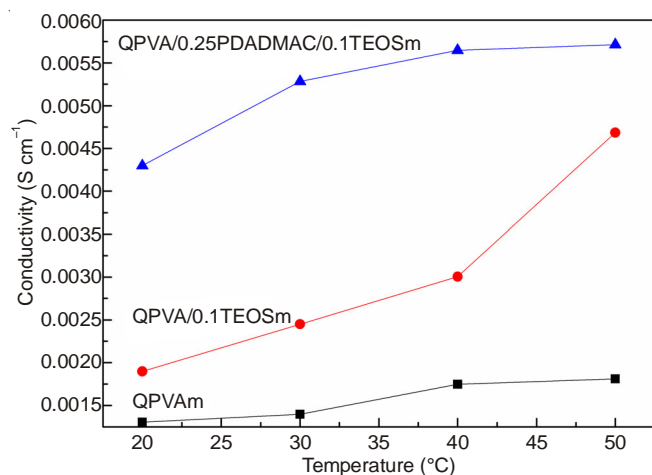


Fig. 7. Relation between temperature and the ionic conductivity of the membranes

Ionic conductivity is hypothesized also to follow the Arrhenius law. The ion transport activation energy E_a of the three effective films can be calculated from the formula $E_a = -b \times R$, where b is the slope of the line fitted by $1000/T$ (K^{-1}) and $\ln(\sigma/S\text{ cm}^{-1})$ and R is the gas constant (8.314 kJ/mol). The E_a of the three effective membranes, namely are 5.209, 12.423 and 4.053 kJ/mol, respectively. QPVA/0.25PDADMAC/0.1TEOSm has the lowest E_a which resulted from its "orange peel-like" structure upon the addition of PDADMAC, thereby causing the easy anion transport. On the other hand, the compact structure of QPVA/0.1TEOSm at low temperature and its high E_a impedes anion transport. The loose segmental structure largely influences ionic conductivity and an abrupt enlargement occurs at high temperature. Hence, the spans of the points on the fitting line amplify naturally and E_a is the maximum (Fig. 8).

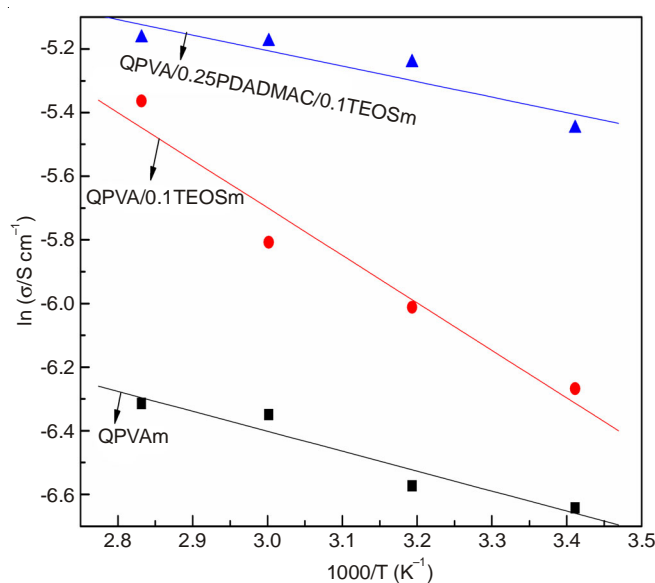


Fig. 8. Ion transfer activation energy E_a fitted by the Arrhenius law.

Conclusion

The new hybrid anion-exchange membranes were prepared with QPVA and PDADMAC through the sol-gel reaction incorporating TEOS. The homogeneous solution was obtained at a mass ratio of QPVA:PDADMAC = 4:1 and pH adjusted to 3. The sol-gel casting solution was reacted with TEOS and cast on the homemade model and dried to get the initial membranes. After cross-linking for 5 h in glutaraldehyde/acetone solution (pH 5, 30 °C), QPVA/0.25PDADMAC/0.1TEOSm was generated. Compared with other membranes, it has an excellent ionic conductivity. Because of its compact structure, its dimensional stability in methanol and thermal resistance are considerable. In particular, its thermal stability reached its maximal value in the range of 65-140 °C, whereas its ionic conductivity attained a value of 1.09 mmol/g. Its methanol permeability decreased to 2.8×10^{-6} cm²/s, which is superior to that of the Nafion-117 membrane ($(4.5-9.2) \times 10^{-6}$ cm²/s). In addition, the membrane also exhibited lower ionic conductivity and higher ion transport activation energy. All these advantages point to its potential applications in ADMFC at low temperature.

REFERENCES

1. D. Xu, Y. Wang, Y. Zhang and G. Zhang, *Chem. Res. Chin. Univ.*, **26**, 6 (2010).
2. H.C. Chiu, C.H. Liu, S.C. Chen and S.Y. Suen, *J. Membr. Sci.*, **337**, 282 (2009).
3. R. Vinodh, R. Padmavathi and D. Sangeetha, *Desalination*, **267**, 267 (2011).
4. T. Chakrabarty, S. Prakash and V.K. Shahi, *J. Membr. Sci.*, **428**, 86 (2013).
5. Y.H. Wu, J.Y. Luo, L.L. Zhao, G.C. Zhang, C.M. Wu and T.W. Xu, *J. Membr. Sci.*, **428**, 95 (2013).
6. T. Uragami, Y. Tanaka and S. Nishida, *Desalination*, **147**, 449 (2002).
7. M.-C. Chang and C.Y. Tai, *Chem. Eng. J.*, **160**, 1 (2010).
8. L.Y. Zhong, J. Scharer, M.M. Young, D. Fenner, L. Crossley, C.H. Honeyman, S.Y. Suen and C.P. Chou, *J. Chromatogr. B*, **879**, 9 (2011).
9. Y.B. Song, L.Z. Zhang, W.P. Gan, J.P. Zhou and L.N. Zhang, *Colloids Surf. B*, **83**, 313 (2011).
10. J. Ran, L. Wu, J.R. Varcoe, A.L. Ong, S.D. Poynton and T.W. Xu, *J. Membr. Sci.*, **415**, 242 (2012).
11. A. Nazir, K. Schroën and R. Boom, *J. Membr. Sci.*, **362**, 1 (2010).
12. J.H. Wang, S.H. Li and S.B. Zhang, *Macromolecules*, **43**, 3890 (2010).
13. Y. Wan, B. Peppley, K.A.M. Creber and V.T. Bui, *J. Power Sources*, **195**, 3785 (2010).
14. J.R. Varcoe and R.C.T. Slade, *Fuel Cells*, **5**, 187 (2005).
15. Q.H. Zeng, Q.L. Liu, I. Broadwell, A.M. Zhu, Y. Xiong and X.P. Tu, *J. Membr. Sci.*, **349**, 237 (2010).
16. G.G. Wang, Y.M. Weng, D. Chu, R.R. Chen and D. Xie, *J. Membr. Sci.*, **332**, 63 (2009).
17. Z.J. Xia, S. Yuan, G.P. Jiang, X.X. Guo, J.H. Fang, L.L. Liu, J.L. Qiao and J. Yin, *J. Membr. Sci.*, **390-391**, 152 (2012).
18. T.J. Clark, N.J. Robertson, H.A. Kostalik IV, E.B. Lobkovsky, P.F. Mutolo, H.D. Abruña and G.W. Coates, *J. Am. Chem. Soc.*, **131**, 12888 (2009).
19. H.A. Kostalik IV, T.J. Clark, N.J. Robertson, P.F. Mutolo, J.M. Longo, H.D. Abruña and G.W. Coates, *Macromolecules*, **43**, 7147 (2010).
20. Y. Xiong, J. Fang, Q.H. Zeng and Q.L. Liu, *J. Membr. Sci.*, **311**, 319 (2008).
21. Y. Xiong, Q.L. Liu, Q.G. Zhang and A.M. Zhu, *J. Power Sources*, **183**, 447 (2008).
22. Y. Xiong, Q.L. Liu, A.M. Zhu, S.M. Huang and Q.H. Zeng, *J. Power Sources*, **186**, 328 (2009).
23. P.R. Meng, L.B. Li, H.X. Qin, X.C. Liu and C.X. Chen, *J. Chem. Ind. Eng.*, **57**, 7 (2006).
24. J. Fu, J.L. Qiao and J.X. Ma, *Chem. J. Chinese Univ.*, **32**, 7 (2011).
25. J. Fu, R. Lin, H. Lv, X.L. Wang, J.X. Ma and J.L. Qiao, *Acta Phys. Chim. Sin.*, **26**, 10 (2010).
26. N. Jiang, Y.G. Shen, H.J. Zhang, S.N. Bao and X.Y. Hou, *Polym. Mater. Sci. Eng.*, **22**, 135 (2006).
27. J. Fang and P.K. Shen, *J. Membr. Sci.*, **285**, 317 (2006).
28. Y.S. Kim, M.A. Hickner, L.M. Dong, B.S. Pivovar and J.E. McGrath, *J. Membr. Sci.*, **243**, 317 (2004).
29. Y. Xiong, Q.-L. Liu, A.-M. Zhu, S.M. Huang and Q.-H. Zeng, *J. Power Sources*, **186**, 328 (2009).